Published in final edited form as:
Mov Disord. 2014 March ; 29(0 3): 396–401. doi:10.1002/mds.25591.

Elevated Arteriolar Cerebral Blood Volume in Prodromal Huntington's Disease

Jun Hua, Ph.D.[1,2,*], **Paul G. Unschuld, M.D.**[3,4,*], **Russell L. Margolis, M.D.**[3,5], **Peter C. M. van Zijl, Ph.D.**[1,2], and **Christopher A. Ross, M.D., Ph.D.**[3,5,6]

[1]The Russell H. Morgan Department of Radiology and Radiological Science, Division of MR Research, The Johns Hopkins University School of Medicine, Baltimore, MD USA [2]F.M. Kirby Research Center for Functional Brain Imaging, Kennedy Krieger Institute, Baltimore, MD USA [3]Department of Psychiatry, Johns Hopkins University School of Medicine, Baltimore, Maryland, USA [4]Division of Psychiatry Research and Psychogeriatric Medicine, University of Zürich, Switzerland [5]Department of Neurology, and Program in Cellular and Molecular Medicine, Johns Hopkins University School of Medicine, Baltimore, Maryland, USA [6]Departments of Neuroscience and Pharmacology, Johns Hopkins University School of Medicine, Baltimore, Maryland, USA

Abstract

Background—Neurovascular alterations have been implicated in the pathophysiology of Huntington's Disease (HD). As arterioles are most responsive to metabolic alterations, arteriolar-cerebral-blood-volume (CBV_a) is an important indicator of cerebrovascular regulation. This pilot

Corresponding Author: Jun Hua, Department of Radiology, Johns Hopkins University School of Medicine, F.M. Kirby Research Center for Functional Brain Imaging, Kennedy Krieger Institute, 707 N Broadway, Baltimore, MD, 21205, jhua@mri.jhu.edu; Tel: 443-923-9513; Fax: 443-923-9505.
*J.H. and P.G.U. contributed equally to this work.

Financial disclosure related to research covered in this article:
Dr. Hua reports no disclosures.
Dr. Unschuld reports no disclosures.
Dr. Margolis reports no disclosures.
Dr. van Zijl has a patent on VASO technology licensed to Philips Healthcare.
Dr. Ross reports no disclosures.

Author Roles:

1. Research project:
   - **A.** Conception: J.H., P.G.U., R.L.M., P.C.M.VZ, and C.A.R.;
   - **B.** Organization and Execution: J.H. and P.G.U.;
2. Statistical Analysis: J.H. and P.G.U.;
3. Manuscript Preparation:
   - **A.** Writing of the first draft: J.H.;
   - **B.** Review and Critique: P.G.U., R.L.M., P.C.M.VZ, and C.A.R.

Full financial disclosure for the previous 12 months:
Dr. Hua reports no disclosures.
Dr. Unschuld reports no disclosures.
Dr. Margolis reports no disclosures.
This study was performed on a human MRI scanner manufactured by Philips Healthcare. Dr. van Zijl is a paid lecturer and has a grant from Philips Healthcare. He also is the inventor of technology licensed to Philips. This arrangement has been approved by Johns Hopkins University in accordance with its conflict of interest policies.
Dr. Ross reports no disclosures.

study is intended to investigate potential neurovascular (CBV_a) abnormality in prodromal-HD, and compare it with the widely used imaging marker brain atrophy.

Methods—CBV_a and brain volumes were measured with ultra-high field (7T) magnetic-resonance-imaging in seven prodromal-HD patients and nine age-matched controls.

Results—Cortical CBV_a was significantly elevated in prodromal-HD patients (relative difference=38.5%, effect size=1.48). Significant correlations were found between CBV_a in frontal cortex and genetic measures. By contrast, no significant brain atrophy was detected in these prodromal-HD patients.

Conclusions—CBV_a may be abnormal in prodromal-HD, even before substantial brain atrophy occurs. Further investigation with a larger cohort and longitudinal follow-up is merited to determine whether it could be used as a potential biomarker for clinical trials.

Keywords

neurovascular; neurodegeneration; atrophy; imaging; biomarker

Introduction

Huntington's Disease (HD) is a neurodegenerative disorder caused by a CAG-repeat expansion in the *Huntingtin* gene, and characterized by progressive deficits in motor, psychiatric, cognitive and behavioral function. During the prodromal period (starting about 15 years prior to onset of motor symptoms), subtle brain changes begin, as well as very subtle cognitive and motor function alterations[1–3]. A major goal for the treatment of HD will be to design neuroprotective therapies during the prodromal and early phases of the disorder. However, such therapeutic trials are hampered by the lack of sensitive and reversible early biomarkers for HD, particularly in the prodromal period[1–3].

Regional brain atrophy begins in striatum and cortex many years before the onset of diagnosable symptoms in HD[1–4]. Functional brain changes[5,6] suggest that neuronal dysfunction, perhaps related to neurovascular and metabolic alterations, may be early features of the disorder. It is therefore important to investigate potential microvascular abnormality in the prodromal period. Perturbations in cerebral glucose metabolism[7–15] and cerebral blood flow (CBF)[15–19] have been found in HD patients. Changes in microvasculature have been observed with histology in the YAC128 mouse model of HD[20], suggesting that blood volume alterations could be present in HD. Two recent imaging studies reported elevated cerebral blood volume (CBV) in brain regions in the R6/2 mouse model of HD[13,21]. Whether such microvascular abnormality occurs in the prodromal phase in HD patients, however, is unknown. Neurophysiology studies have shown that small arteries and arterioles are most responsive to changes in metabolism[22–25]. Therefore, arteriolar CBV (CBV_a) may be more sensitive than total CBV as an indicator for the homeostasis of the microvasculature.

In this study, we applied the inflow-based vascular-space-occupancy (iVASO) technique[26–28], a non-invasive magnetic resonance imaging (MRI) method, at ultra-high field (7T), to investigate potential CBV_a abnormality in cortical gray matter in prodromal-HD patients, and compare it with the widely used imaging marker brain atrophy in the same subjects.

Methods

Seven prodromal-HD patients and nine sex- and age-matched controls were recruited, and gave written informed consent before participating in this Johns Hopkins Institutional

Review Board approved study. Demographic data and clinical measures are summarized in table e-1 (appendix). No subject had other neurologic history or signs on exam, or history of stroke or other vascular diseases. The sample size was estimated based on the effect size (>2.3) of CBV increase from two recent imaging studies in the R6/2 mouse model of HD[13,21] to ensure a power of 0.8 and significance at α=0.05.

MRI scans were performed on a Philips 7T human scanner. Whole-brain anatomical images were acquired with a high-resolution magnetization-prepared-rapid-acquisition-gradient-echo (MPRAGE) scan. CBV_a was measured using iVASO-MRI[27] with a single slice oriented oblique axial, slightly above the ventricle in order to sample all lobes of cerebral cortex. The slice was carefully prescribed on the MPRAGE images, and centered on the line through the superior edge of corpus callosum and the posterior end of calcarine fissure. iVASO-MRI employs a spatially selective inversion to zero out (null) the arterial blood signal. By comparing to a control scan without blood nulling, CBV_a can be calculated from the difference signal. To account for the heterogeneity of vascular transit times, interleaved nulling and control images are acquired at multiple post-inversion delay times, from which absolute CBV_a and arterial transit time can be quantified using the iVASO theory[27]. Moreover, crushing gradients can be incorporated to suppress signals from fast flowing blood in large arteries, thereby sensitizing this method to CBV_a predominantly in the arterioles[27]. Imaging parameters are summarized in appendix e-1.

To minimize motion-related image artifacts, foam pads and straps were used to restrict head movement during MRI scans. HD patients were all in prodromal phase and involuntary movements were minimal. No major image artifacts due to subject movement during the image acquisition period (about 30ms for each iVASO image, appendix e-1) were seen.

Image analysis was performed with SPM8 (http://www.fil.ion.ucl.ac.uk/spm/) and Matlab6 (Mathworks). iVASO images were re-aligned using the routine in SPM8 to correct for head movement between scans. The nulling and control iVASO images were processed with the surround subtraction method[27] to calculate the difference signals, from which CBV_a and arterial transit time maps were numerically fitted with the iVASO equations[27]. Anatomical images were co-registered with iVASO images using the mutual information algorithm in SPM8. Partial volume effects on the iVASO signals in gray matter were corrected[29]. The iVASO slice was partitioned into three regions: frontal, occipital, and parietal&temporal, as guided by the central, lateral and parietal-occipital sulci. Volumes of brain regions were derived from tissue segmentation of the high resolution MPRAGE scans using TOpology-preserving, Anatomy-Driven Segmentation (TOADS)[30].

Both parametric and non-parametric (for small sample size) methods were used for statistical analysis. Group differences were assessed using *t*-Test and Wilcoxon-rank-sum-test. Multiple comparisons were corrected with false-discovery-rate. Effect sizes were estimated with Cohen's *d*. Correlations were tested using: 1) Pearson-correlation-coefficient (r); 2) Spearman-rank-correlation-coefficient (r_s); 3) adjusted-R2 from simple and multiple (covariate-age) linear regression. Correlations between CBV_a and genetic measures including the CAG-Age product (CAP) score[31] and estimated years-to-onset (YTO)[32] of motor symptoms were tested. Both the CAP-score and YTO are based on two key observables: CAG-repeat length and age, and thus are considered better metrics for disease progression than either of the two alone.

Results

Representative CBV_a maps are shown in Figure 1a. Gray matter CBV_a (Figure 1b) was significantly greater in prodromal-HD patients in the whole slice, frontal and

parietal&temporal cortex, with relative difference ([HD-control]/control) of 30–50% and effect sizes of 1.4–2.1 (table e-2 in appendix). This effect was the most significant in the frontal cortex (relative difference=48.9%, effect size=2.11). Similar trend was observed in the occipital cortex. Gray matter CBV_a in controls were all in normal range[27]. Arterial transit times were slightly longer in prodromal-HD patients, but the differences were not statistically significant except in the occipital lobe (table e-3). Average motion during iVASO scans were quantified in SPM8 realignment routine (control: 0.35±0.18mm translation, 0.05±0.06º rotation; prodromal-HD: 0.31±0.15mm translation, 0.05±0.05º rotation; mean±SD, $P>0.1$). The CBVa difference remains significant ($P<0.05$) in whole-slice, frontal, and parietal&temporal lobes after controlling for the average motion parameters as confounding covariates. A potential sex difference in CBV_a was assessed by combining the data from a previous CBV_a study in normal subjects[27] and the control subjects in this study: a total of 9 female (45±10) and 9 male (43±12) age-matched normal subjects. No significant difference was found (female: 1.36±0.27ml/100ml, male: 1.33±0.31ml/100ml, n=9, $P>0.1$).

Significant correlations (adjusted-$R^2>0.5$ and $P<0.05$) were found between gray matter CBV_a in frontal cortex and genetic measures including the CAP-score and estimated YTO (Figure 2, table e-4 in appendix). No significant impact from age was detected when performing multiple linear regression with both CBV_a and age as independent variables. Similar trends of correlations between gray matter CBV_a in other cortical regions or arterial transit times and CAP/YTO were observed, but did not reach statistical significance (adjusted-R^2=0.3–0.6 but $P>0.1$).

No significant atrophy was found in any brain regions (table e-5 in appendix) including cortical gray matter and striatum (caudate and putamen) in this small group of prodromal-HD patients. The relative volume differences between patients and controls were 3–11% (except ventricles, 34.7%, but $P=0.45$), and the effects sizes were 0.10–0.89, smaller than CBV_a. No significant correlation was found between any of the brain volumes and CAP/YTO, or between brain volumes and gray matter CBV_a.

Discussion

We found that cortical gray matter CBV_a was significantly elevated in prodromal-HD patients compared to age-matched controls. This is, to our knowledge, the first study to examine CBV_a, which is the most actively regulated compartment of the microvasculature, in prodromal-HD patients.

Our finding is congruent with studies of post-mortem brain tissue from HD patients[33], and of striatum of the YAC128 mouse model of HD[20], which reported slightly decreased microvessel diameter but significantly increased vessel density and length, implying larger total CBV. Cepeda-Prado et al[13] reported increased total CBV in prefrontal, primary motor, and temporal cortex, and striatum in the R6/2 mouse model of HD. Lin et al[21] visualized abnormal microvasculature in R6/2 mice with a contrast-enhanced angiography method, and measured larger total CBV in neocortex and striatum compared to controls. These data are all consistent with our finding of enlarged CBV_a in prodromal-HD patients.

CBV_a was elevated most significantly in frontal cortex, which has a significant projection from the striatum. Neurovascular abnormalities in striatum[7–13,15–19] and pallidum[19,34,35] have been reported in prodromal and early HD patients, which may be linked to the increase of GABA (gamma-aminobutyric acid) receptors and loss of GABAergic neurons in the globus pallidus in HD[19,36].

CBF abnormality in HD has been reported in many studies[15–19]. CBF and CBV are two complementary measures for the microvasculature[37,38], which can be uncoupled under pathological conditions such as ischemia and tumors. Arterial microvessels (CBV_a) are the primary regulators of cerebral perfusion[22–25]. Our data show a larger difference between prodromal-HD and control subjects in cortical CBV_a (30–50%) than cortical CBF (15–20%) reported in a recent study on early-HD patients[19]. This suggests that CBV_a may be a useful alternative measure for detecting microvascular abnormality in HD in certain brain regions.

Further study, however, is needed to elucidate mechanisms, and determine whether there is a primary vascular impairment, or an effect on vascular reactivity secondary to mitochondrial dysfunction and metabolic disturbances. Elevated levels of vascular-endothelial-growth-factor (VEGF), a protein produced by cells that stimulates angiogenesis and regulates vessel growth, have been observed in mutant *huntingtin* striatal cells[39], raising the possibility of primary vascular abnormalities.

The cortical gray matter CBV_a values in prodromal-HD patients correlated with the CAP-score and projected years-to-onset. The CAP-score is an estimate of cumulative toxicity of mutant *Huntingtin* in HD patients[31]. Such correlation suggests that CBV_a could be a biomarker for tracking disease progression in HD.

The fact that no significant brain atrophy, or correlation between CBV_a and brain volumes were found in this small sample of prodromal-HD patients suggests that CBV_a alteration may precede or have a greater magnitude compared to structural changes in HD. Neurovascular defects have been reported in many other neurodegenerative diseases, and have been suggested to be a common feature for neurodegeneration[40]. While reduced blood volume is usually seen in many of these diseases, the elevated CBV_a found here might suggest some unique aspects of pathophysiology in prodromal-HD.

Limitations of this pilot study include the small sample size and the cross-sectional design. Therefore, we adopted statistical methods specifically designed for small sample size. Note that the sample size was estimated based on the effect size of CBV change reported in animal studies[13,21]. As this is the first report on CBV_a abnormality in prodromal-HD patients, our data can be used for more accurate power and sample size calculations for future studies. Another limitation is that the spatial coverage in the brain was restrained to a single slice through the cortex due to technical constraints including limited coil coverage for homogeneous inversion region below the imaging volume in iVASO, not allowing the striatum to be included in this pilot study. Efforts to expand the iVASO method to whole brain coverage are underway.

In summary, our data indicate that CBV_a may be abnormal in prodromal-HD. Further investigation with a larger cohort and longitudinal follow-up is merited to determine the onset and characterize the progression of CBV_a alteration during the prodromal and early phases of HD, and to determine whether it could be used as a potential biomarker for clinical studies and therapeutic trials.

Supplementary Material

Refer to Web version on PubMed Central for supplementary material.

Acknowledgments

The authors thank Joseph Gillen, Terri Brawner, Kathleen Kahl, and Ivana Kusevic (F.M. Kirby Research Center) for experimental assistance and Nadine Yoritomo and Morgan Withenour (Baltimore Huntington's Disease Center) for support in the study organization, and Guillermo Verduzco (Division of Psychiatric Neuroimaging) for technical

assistance. We also thank Dr. Chien-Yuan Lin (University of Texas Southwestern Medical Center, Dallas) for stimulating discussions. This study was supported by the Johns Hopkins Brain Science Institute (BSI), NINDS NS016375, P50AG005146, resource grant P41 EB015909 and a grant from Philips Healthcare. Dr. Paul Unschuld was supported by NIH-T32MH015330.

Study funding: This study was supported by the Johns Hopkins Brain Science Institute (BSI), NIH NINDS NS016375, P50AG005146 and resource grant P41 EB015909. Dr. Unschuld was supported by NIH-T32MH015330.

References

1. Paulsen JS, Nopoulos PC, Aylward E, et al. Striatal and white matter predictors of estimated diagnosis for Huntington disease. Brain Res Bull. 2010; 82(3–4):201–207. [PubMed: 20385209]
2. Tabrizi SJ, Scahill RI, Durr A, et al. Biological and clinical changes in premanifest and early stage Huntington's disease in the TRACK-HD study: the 12-month longitudinal analysis. Lancet Neurol. 2011; 10(1):31–42. [PubMed: 21130037]
3. Tabrizi SJ, Reilmann R, Roos RA, et al. Potential endpoints for clinical trials in premanifest and early Huntington's disease in the TRACK-HD study: analysis of 24 month observational data. Lancet Neurol. 2012; 11(1):42–53. [PubMed: 22137354]
4. Aylward EH, Nopoulos PC, Ross CA, et al. Longitudinal change in regional brain volumes in prodromal Huntington disease. J Neurol Neurosurg Psychiatry. 2011; 82(4):405–410. [PubMed: 20884680]
5. Zimbelman JL, Paulsen JS, Mikos A, Reynolds NC, Hoffmann RG, Rao SM. fMRI detection of early neural dysfunction in preclinical Huntington's disease. J Int Neuropsychol Soc. 2007; 13(5): 758–769. [PubMed: 17697407]
6. Wolf RC, Sambataro F, Vasic N, et al. Longitudinal functional magnetic resonance imaging of cognition in preclinical Huntington's disease. Exp Neurol. 2011; 231(2):214–222. [PubMed: 21726553]
7. Ciarmiello A, Cannella M, Lastoria S, et al. Brain white-matter volume loss and glucose hypometabolism precede the clinical symptoms of Huntington's disease. J Nucl Med. 2006; 47(2): 215–222. [PubMed: 16455626]
8. Feigin A, Leenders KL, Moeller JR, et al. Metabolic network abnormalities in early Huntington's disease: an [(18)F]FDG PET study. J Nucl Med. 2001; 42(11):1591–1595. [PubMed: 11696626]
9. Kuwert T, Noth J, Scholz D, et al. Comparison of somatosensory evoked potentials with striatal glucose consumption measured by positron emission tomography in the early diagnosis of Huntington's disease. Mov Disord. 1993; 8(1):98–106. [PubMed: 8419813]
10. Sax DS, Powsner R, Kim A, et al. Evidence of cortical metabolic dysfunction in early Huntington's disease by single-photon-emission computed tomography. Mov Disord. 1996; 11(6): 671–677. [PubMed: 8914093]
11. Antonini A, Leenders KL, Spiegel R, et al. Striatal glucose metabolism and dopamine D2 receptor binding in asymptomatic gene carriers and patients with Huntington's disease. Brain. 1996; 119 (Pt 6):2085–2095. [PubMed: 9010012]
12. Powers WJ, Videen TO, Markham J, et al. Selective defect of in vivo glycolysis in early Huntington's disease striatum. Proc Natl Acad Sci U S A. 2007; 104(8):2945–2949. [PubMed: 17299049]
13. Cepeda-Prado E, Popp S, Khan U, et al. R6/2 Huntington's disease mice develop early and progressive abnormal brain metabolism and seizures. J Neurosci. 2012; 32(19):6456–6467. [PubMed: 22573668]
14. Eidelberg D. Metabolic brain networks in neurodegenerative disorders: a functional imaging approach. Trends Neurosci. 2009; 32(10):548–557. [PubMed: 19765835]
15. Ma Y, Eidelberg D. Functional imaging of cerebral blood flow and glucose metabolism in Parkinson's disease and Huntington's disease. Mol Imaging Biol. 2007; 9(4):223–233. [PubMed: 17334854]
16. Deckel AW, Weiner R, Szigeti D, Clark V, Vento J. Altered patterns of regional cerebral blood flow in patients with Huntington's disease: a SPECT study during rest and cognitive or motor activation. J Nucl Med. 2000; 41(5):773–780. [PubMed: 10809191]

17. Harris GJ, Codori AM, Lewis RF, Schmidt E, Bedi A, Brandt J. Reduced basal ganglia blood flow and volume in pre-symptomatic, gene-tested persons at-risk for Huntington's disease. Brain. 1999; 122 (Pt 9):1667–1678. [PubMed: 10468506]
18. Wolf RC, Gron G, Sambataro F, et al. Magnetic resonance perfusion imaging of resting-state cerebral blood flow in preclinical Huntington's disease. J Cereb Blood Flow Metab. 2011; 31(9): 1908–1918. [PubMed: 21559028]
19. Chen JJ, Salat DH, Rosas HD. Complex relationships between cerebral blood flow and brain atrophy in early Huntington's disease. Neuroimage. 2012; 59(2):1043–1051. [PubMed: 21945790]
20. Franciosi S, Ryu JK, Shim Y, et al. Age-dependent neurovascular abnormalities and altered microglial morphology in the YAC128 mouse model of Huntington disease. Neurobiol Dis. 2012; 45(1):438–449. [PubMed: 21946335]
21. Lin, C.; Huang, C.; Lin, M., et al. Magnetic Resonance Microscopic Angiography Visualization of Abnormal Microvasculature in a Transgenic Mouse Model of Huntington's Disease. Proc 18th Annual Meeting ISMRM; 2010; Stockholm, Sweden. 2010. p. 462
22. Iadecola C, Nedergaard M. Glial regulation of the cerebral microvasculature. Nat Neurosci. 2007; 10(11):1369–1376. [PubMed: 17965657]
23. Ito H, Ibaraki M, Kanno I, Fukuda H, Miura S. Changes in the arterial fraction of human cerebral blood volume during hypercapnia and hypocapnia measured by positron emission tomography. J Cereb Blood Flow Metab. 2005; 25(7):852. [PubMed: 15716851]
24. Kim T, Hendrich KS, Masamoto K, Kim SG. Arterial versus total blood volume changes during neural activity-induced cerebral blood flow change: implication for BOLD fMRI. J Cereb Blood Flow Metab. 2007; 27(6):1235. [PubMed: 17180136]
25. Takano T, Tian GF, Peng W, et al. Astrocyte-mediated control of cerebral blood flow. Nat Neurosci. 2006; 9(2):260. [PubMed: 16388306]
26. Hua J, Qin Q, Donahue MJ, Zhou J, Pekar JJ, van Zijl PC. Inflow-based vascular-space-occupancy (iVASO) MRI. Magn Reson Med. 2011; 66(1):40–56. [PubMed: 21695719]
27. Hua J, Qin Q, Pekar JJ, Zijl PC. Measurement of absolute arterial cerebral blood volume in human brain without using a contrast agent. NMR Biomed. 2011; 24(10):1313–1325. [PubMed: 21608057]
28. Donahue MJ, Sideso E, MacIntosh BJ, Kennedy J, Handa A, Jezzard P. Absolute arterial cerebral blood volume quantification using inflow vascular-space-occupancy with dynamic subtraction magnetic resonance imaging. J Cereb Blood Flow Metab. 2010; 30(7):1329–1342. [PubMed: 20145656]
29. Johnson NA, Jahng GH, Weiner MW, et al. Pattern of cerebral hypoperfusion in Alzheimer disease and mild cognitive impairment measured with arterial spin-labeling MR imaging: initial experience. Radiology. 2005; 234(3):851–859. [PubMed: 15734937]
30. Bazin PL, Pham DL. Topology-preserving tissue classification of magnetic resonance brain images. IEEE Trans Med Imaging. 2007; 26(4):487–496. [PubMed: 17427736]
31. Zhang Y, Long JD, Mills JA, Warner JH, Lu W, Paulsen JS. Indexing disease progression at study entry with individuals at-risk for Huntington disease. Am J Med Genet B Neuropsychiatr Genet. 2011; 156B(7):751–763. [PubMed: 21858921]
32. Langbehn DR, Brinkman RR, Falush D, Paulsen JS, Hayden MR. A new model for prediction of the age of onset and penetrance for Huntington's disease based on CAG length. Clin Genet. 2004; 65(4):267–277. [PubMed: 15025718]
33. Vis JC, Nicholson LF, Faull RL, Evans WH, Severs NJ, Green CR. Connexin expression in Huntington's diseased human brain. Cell Biol Int. 1998; 22(11–12):837–847. [PubMed: 10873295]
34. Politis M, Pavese N, Tai YF, et al. Microglial activation in regions related to cognitive function predicts disease onset in Huntington's disease: a multimodal imaging study. Hum Brain Mapp. 2011; 32(2):258–270. [PubMed: 21229614]
35. van den Bogaard SJ, Dumas EM, Acharya TP, et al. Early atrophy of pallidum and accumbens nucleus in Huntington's disease. J Neurol. 2011; 258(3):412–420. [PubMed: 20936300]

36. Allen KL, Waldvogel HJ, Glass M, Faull RL. Cannabinoid (CB(1)), GABA(A) and GABA(B) receptor subunit changes in the globus pallidus in Huntington's disease. J Chem Neuroanat. 2009; 37(4):266–281. [PubMed: 19481011]

37. Rostrup E, Knudsen GM, Law I, Holm S, Larsson HB, Paulson OB. The relationship between cerebral blood flow and volume in humans. Neuroimage. 2005; 24(1):1–11. [PubMed: 15588591]

38. Hua J, Stevens RD, Huang AJ, Pekar JJ, van Zijl PC. Physiological origin for the BOLD poststimulus undershoot in human brain: vascular compliance versus oxygen metabolism. J Cereb Blood Flow Metab. 2011; 31(7):1599–1611. [PubMed: 21468090]

39. Niatsetskaya Z, Basso M, Speer RE, et al. HIF prolyl hydroxylase inhibitors prevent neuronal death induced by mitochondrial toxins: therapeutic implications for Huntington's disease and Alzheimer's disease. Antioxid Redox Signal. 2010; 12(4):435–443. [PubMed: 19659431]

40. Zacchigna S, Lambrechts D, Carmeliet P. Neurovascular signalling defects in neurodegeneration. Nat Rev Neurosci. 2008; 9(3):169–181. [PubMed: 18253131]

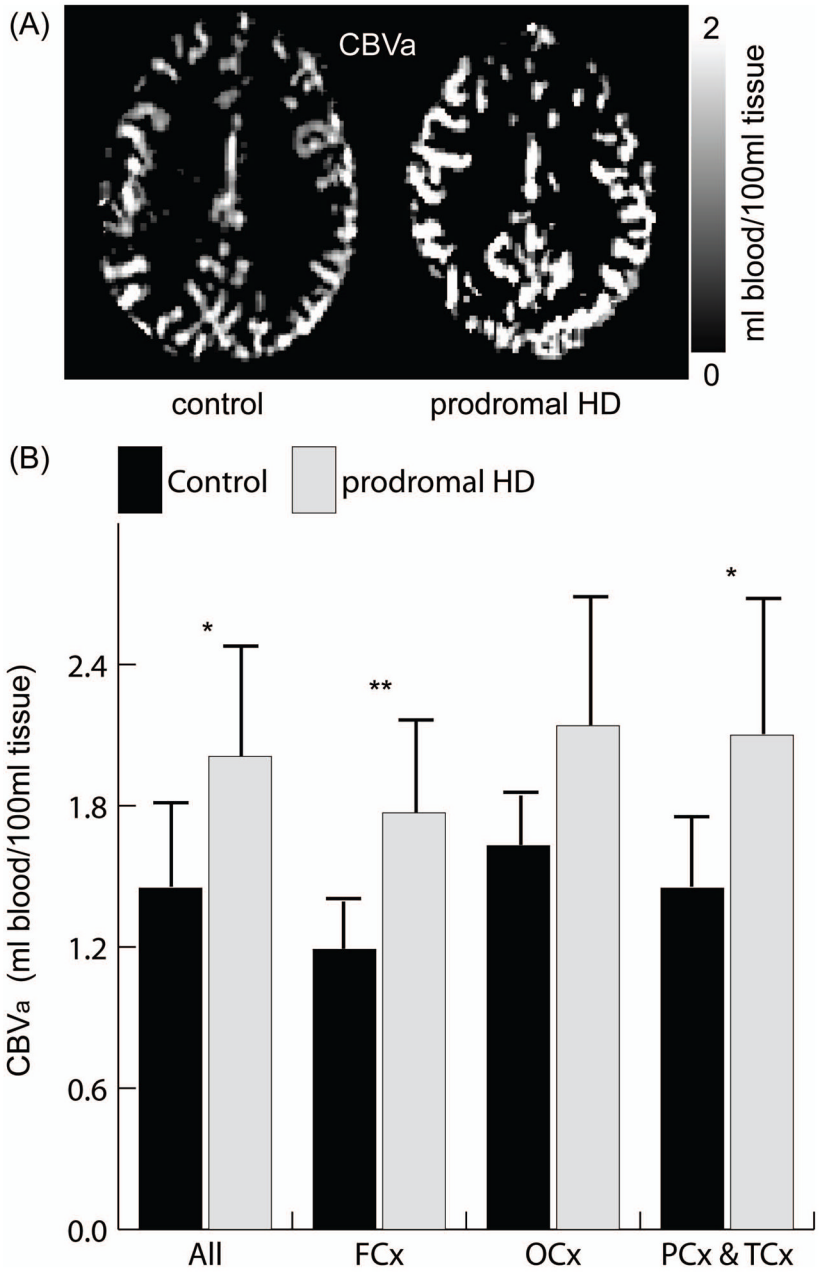

Figure 1.

Typical CBV_a maps (A) and average gray matter CBV_a (B) in the whole slice (All), frontal (FCx), occipital (OCx), and parietal&temporal (PCx&TCx) cortex. Errorbars: standard deviations. P-values from Wilcoxon-rank-sum-test, adjusted for multiple comparisons (table e-2). *, P<0.05, **, P<0.01.

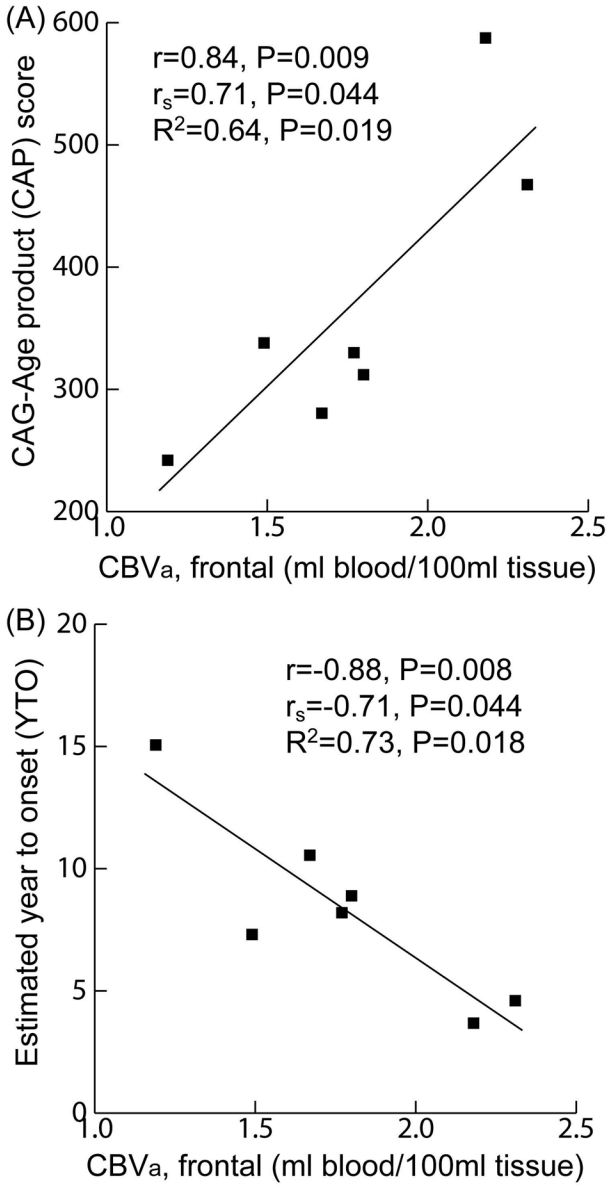

Figure 2.

Correlations analysis. Scatter plots showing correlations between gray matter CBV_a in frontal cortex and CAP score (A) and YTO (B) in prodromal-HD patients. r: Pearson-correlation-coefficient; r_s: Spearman-rank-correlation-coefficient; R^2: adjusted R^2 from simple linear regression. P-values adjusted for multiple comparisons.